Numerical analyses of cement-based piezoelectric smart composites

†*Jan Sladek[1], Pavol Novak[2], Peter L. Bishay[3], and Vladimir Sladek[1]

[1]Institute of Construction and Architecture, Slovak Academy of Sciences, 84503 Bratislava, Slovakia.
[2]Faculty of Mechanical Engineering, University of Zilina, Slovakia
[3]College of Engineering and Computer Science, California State University, Northridge, USA.

*Presenting author: jan.sladek@savba.sk
†Corresponding author: jan.sladek@savba.sk

Abstract

Smart cement-based composite materials have great potential to be used in structural health monitoring (SHM) systems. In this work, the effective thermo-electro-mechanical material properties of cement-based piezoelectric smart composites are characterized. The homogenization techniques are applied on a representative volume element (RVE), where a typical distribution of piezoelectric 3-D particles in the cement matrix is considered. The finite element method (FEM) is used to solve sets of different boundary value problems for the RVE to get the effective thermo-electro-mechanical properties. The effect of the particle volume fraction on the effective composite properties is investigated.

Keywords: **3-D piezoelectric particles, cement matrix, volume fraction, effective material properties, finite element method**

Introduction

Reinforced concrete made from cement-based materials is the most popular materials used for larger civil engineering structures. However, this material is not convenient for structural health monitoring (SHM) systems to prevent catastrophic failure of civil structures. To have this possibility for civil structures, cement-based composites with piezoelectric properties need to be developed. Normal mixing and spread techniques were utilized to produce cement-based piezoelectric smart composite [1-4]. Published technical papers on the effect of volume fraction of particles and their size on the properties of the PZT–cement based composites are still very limited in the literature and are mostly based on experimental approaches.

The goal of the present paper is to provide an efficient computational tool for evaluating the effective material properties of PZT–cement based composites. Numerical analyses are performed on a representative volume element (RVE), which contains essential physical geometrical information about the microstructural components represented by the PZT particles in the cement matrix. The computational thermal homogenization, applied to the microscale and mesoscale of concrete sequentially in [5], is extended to the PZT–cement based composites. The finite element model of the RVE is developed to solve boundary value problems with different boundary conditions in order to evaluate the effective thermo-electro-mechanical properties of PZT cement-based composites. These results have not been reported in the literature, according to the best of the authors' knowledge.

Thermal homogenization of smart concrete

Consider a periodic distribution of 3D piezoelectric particles in a cement matrix, and for the numerical simulation, we select a representative volume element (RVE) as shown in Figure 1.

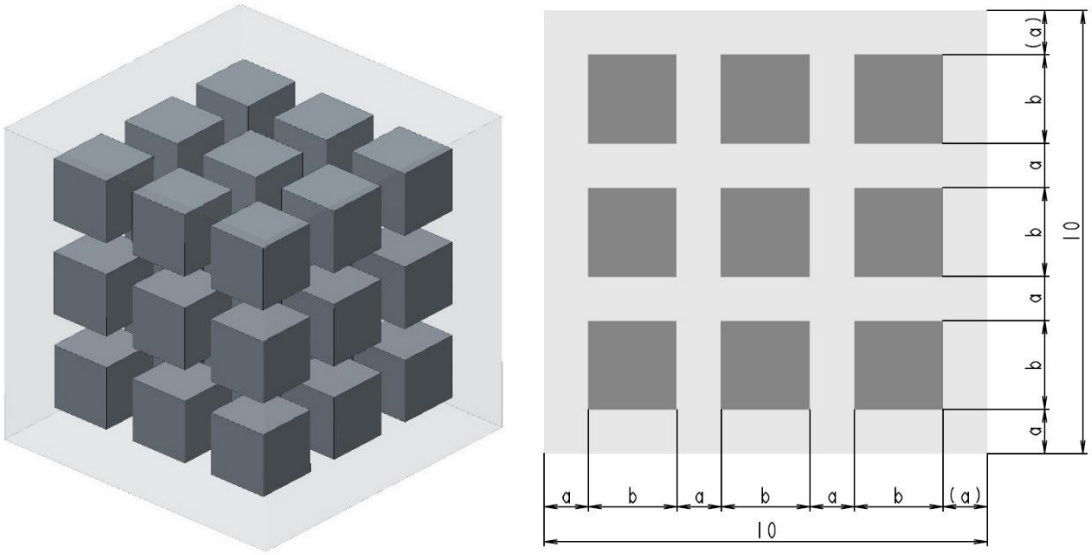

Figure 1. The RVE of a piezoelectric cement composite

The governing equations of the thermo-piezoelectricity consist of Maxwell's equations, the heat conduction equation and the balance of momentum [6]:

$$\sigma_{ij,j}(\mathbf{x}) = 0; \qquad D_{i,i}(\mathbf{x}) = 0; \qquad \psi_{i,i}(\mathbf{x}) = 0, \tag{1}$$

where σ_{ij} , D_i and ψ_i are the stress tensor, electric displacement vector and heat flux vector, respectively. $\mathbf{x}$ is the position vector. The strain tensor ε_{ij} and the electric field vector E_j are related to the mechanical displacement vector u_i and the scalar electric potential ϕ , respectively, by

$$\varepsilon_{ij} = \frac{1}{2}\left(u_{i,j} + u_{j,i}\right); \qquad E_j = -\phi_{,j}\,. \tag{2}$$

The constitutive equations express coupling of the mechanical, electrical and thermal fields:

$$\sigma_{ij}(\mathbf{x}) = c_{ijkl}\varepsilon_{kl}(\mathbf{x}) - e_{kij}E_k(\mathbf{x}) - \gamma_{ij}\theta(\mathbf{x}); \qquad D_i(\mathbf{x}) = e_{ijk}\varepsilon_{ik}(\mathbf{x}) + h_{ij}E_j(\mathbf{x}) + p_i\theta(\mathbf{x}), \tag{3}$$

where c_{ijkl} , e_{ijk} , h_{ij} and p_i are the elastic, piezoelectric, dielectric and pyroelectric material tensors in a thermal piezoelectric medium, respectively. θ is the temperature difference. The stress-temperature moduli γ_{ij} are expressed as functions of the elastic stiffness coefficients and the thermal expansion coefficients α_{kl}: $\gamma_{ij} = c_{ijkl}\alpha_{kl}$.

The constitutive equations can be written in matrix form (using the reduced Voigt notation) as:

$$\begin{bmatrix}\sigma_{11}\\ \sigma_{22}\\ \sigma_{33}\\ \sigma_{23}\\ \sigma_{13}\\ \sigma_{12}\end{bmatrix}=\begin{bmatrix}c_{11} & c_{12} & c_{13} & 0 & 0 & 0\\ c_{12} & c_{11} & c_{23} & 0 & 0 & 0\\ c_{13} & c_{23} & c_{33} & 0 & 0 & 0\\ 0 & 0 & 0 & c_{44} & 0 & 0\\ 0 & 0 & 0 & 0 & c_{44} & 0\\ 0 & 0 & 0 & 0 & 0 & c_{66}\end{bmatrix}\begin{bmatrix}\varepsilon_{11}\\ \varepsilon_{22}\\ \varepsilon_{33}\\ 2\varepsilon_{23}\\ 2\varepsilon_{13}\\ 2\varepsilon_{12}\end{bmatrix}-\begin{bmatrix}e_{11} & 0 & e_{13}\\ 0 & e_{11} & e_{13}\\ e_{13} & e_{13} & e_{33}\\ e_{15} & 0 & 0\\ 0 & e_{15} & 0\\ 0 & 0 & 0\end{bmatrix}\begin{bmatrix}E_1\\ E_2\\ E_3\end{bmatrix}-\begin{bmatrix}\gamma_{11}\\ \gamma_{22}\\ \gamma_{33}\\ 0\\ 0\\ 0\end{bmatrix}\theta\,, \tag{4}$$

$$\begin{bmatrix}D_1\\ D_2\\ D_3\end{bmatrix}=\begin{bmatrix}e_{11} & 0 & e_{13} & e_{15} & e_{15} & 0\\ 0 & e_{11} & e_{13} & e_{15} & e_{15} & 0\\ e_{13} & e_{13} & e_{33} & e_{15} & e_{15} & 0\end{bmatrix}\begin{bmatrix}\varepsilon_{11}\\ \varepsilon_{22}\\ \varepsilon_{33}\\ 2\varepsilon_{23}\\ 2\varepsilon_{13}\\ 2\varepsilon_{12}\end{bmatrix}+\begin{bmatrix}h_{11} & 0 & 0\\ 0 & h_{22} & 0\\ 0 & 0 & h_{33}\end{bmatrix}\begin{bmatrix}E_1\\ E_2\\ E_3\end{bmatrix}+\begin{bmatrix}p_1\\ p_2\\ p_3\end{bmatrix}\theta\,, \tag{5}$$

where

$$\begin{bmatrix}\gamma_{11}\\ \gamma_{22}\\ \gamma_{33}\end{bmatrix}=\begin{bmatrix}c_{11} & c_{12} & c_{13}\\ c_{12} & c_{22} & c_{23}\\ c_{13} & c_{23} & c_{33}\end{bmatrix}\begin{bmatrix}\alpha_{11}\\ \alpha_{22}\\ \alpha_{33}\end{bmatrix}. \tag{6}$$

The thermal constitutive equation (Fourier's law) is given by

$$\psi_i(\mathbf{x})=\kappa_{ij}\beta_j(\mathbf{x});\qquad \text{where}\quad \beta_j=\theta_{,j} \tag{7}$$

with κ_{ij} being the thermal conductivity tensor.

The governing equations (1) can be satisfied in the weak form. The residual form in the analyzed domain V is written as:

$$\int_V\left(\sigma_{ij,j}w_i+D_{i,i}w_\phi+\psi_{i,i}w_T\right)dV=0\,, \tag{8}$$

where w_i, w_ϕ and w_T are arbitrary weighting functions that are assumed to vanish along the boundaries where essential boundary conditions are specified (Γ_u, Γ_p and Γ_θ respectively). In FEM, the generalized primary (mechanical displacements, electric potential and temperature) and secondary (strains, electric field and temperature gradients) field variables, $\tilde{\mathbf{u}}$ and $\tilde{\boldsymbol{\varepsilon}}$ respectively, can be approximated over the domain of each finite element V^e in terms of the nodal degrees of freedom, $\mathbf{q}$, and the corresponding shape functions as

$$\tilde{\mathbf{u}}=\mathbf{N}\mathbf{q};\qquad \tilde{\boldsymbol{\varepsilon}}=\mathbf{B}\mathbf{q}\,, \tag{9}$$

where $\mathbf{N}$ is the shape functions matrix, $\mathbf{B}$ is a matrix that contains derivatives of the shape functions, and $\mathbf{q}=\left[u_1^{(1)}\quad u_2^{(1)}\quad u_3^{(1)}\quad \phi^{(1)}\quad \theta^{(1)}\quad u_1^{(2)}\quad ...\right]^T$ is the nodal degrees of freedom vector in 3D, with superscript (k) indicating node number. The finite element equation is then given by

$$\mathbf{Kq} = \mathbf{f_t}; \qquad \mathbf{K} = \int_{V^e} \left(\mathbf{B}^T \tilde{\mathbf{C}} \mathbf{B} + \mathbf{B}^T \mathbf{G} \mathbf{N} \right) dV; \qquad \mathbf{f_t} = \int_{\Gamma_n} \mathbf{N}^T \tilde{\mathbf{t}} d\Gamma \,, \tag{10}$$

where

$$\boldsymbol{\sigma} = \mathbf{C}\boldsymbol{\varepsilon} + \mathbf{G}\mathbf{u}; \qquad \mathbf{C} = \begin{bmatrix} \mathbf{C} & -\mathbf{e}^T & \mathbf{0} \\ \mathbf{e} & \mathbf{h} & \mathbf{0} \\ \mathbf{0} & \mathbf{0} & \boldsymbol{\kappa} \end{bmatrix}; \qquad \mathbf{G} = \begin{bmatrix} \mathbf{0} & \mathbf{0} & -\boldsymbol{\gamma} \\ \mathbf{0} & \mathbf{0} & \mathbf{p} \\ \mathbf{0} & \mathbf{0} & \mathbf{0} \end{bmatrix}. \tag{11}$$

The composite response is determined by the homogenized composite properties or the effective material properties. The effective material coefficients of the piezoelectric cement composite can be computed from the constitutive equations written for the average values of the secondary fields and the conjugated fields on the RVE sample [7].

Results

Consider a sample of Portland cement matrix with embedded PZT-SH particles. The material coefficients of the PZT-SH can be found in [8]. Portland cement matrix properties are as follows: Young's modulus $E = 1.4 \times 10^{10}\, Nm^{-2}$, Poisson's ratio $\nu = 0.2$, heat conductivity $\kappa = 0.29\, W/m\, deg$, and thermal expansion coefficient $\alpha = 11.10^{-6}\ 1/deg$. Figure 2 and Figure 3 show the effect of the PZT particle volume fraction in the smart composite on the effective elastic and piezoelectric material properties. The volume fraction of the PZT particles is varied from 3% to 60%. One can observe from the figures that as the volume fraction of the PZT ceramic particles increases, the elastic material properties of the composite increase. The absolute value of all piezoelectric coefficients significantly increases as the volume fraction increases. The red point in Figure 2 (right) indicates the values of the effective c_{13} for volume fraction 30% and sample size of 1.85 mm obtained in [9].

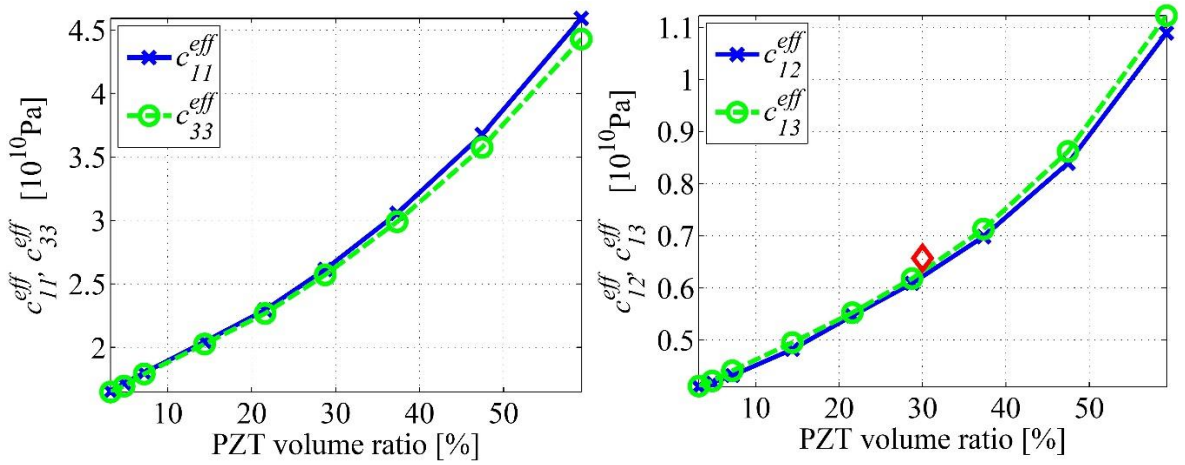

Figure 2. Variation of the effective (left) c_{11} and c_{33}, (right) c_{12} and c_{13} with PZT volume fraction in the smart ceramic composite

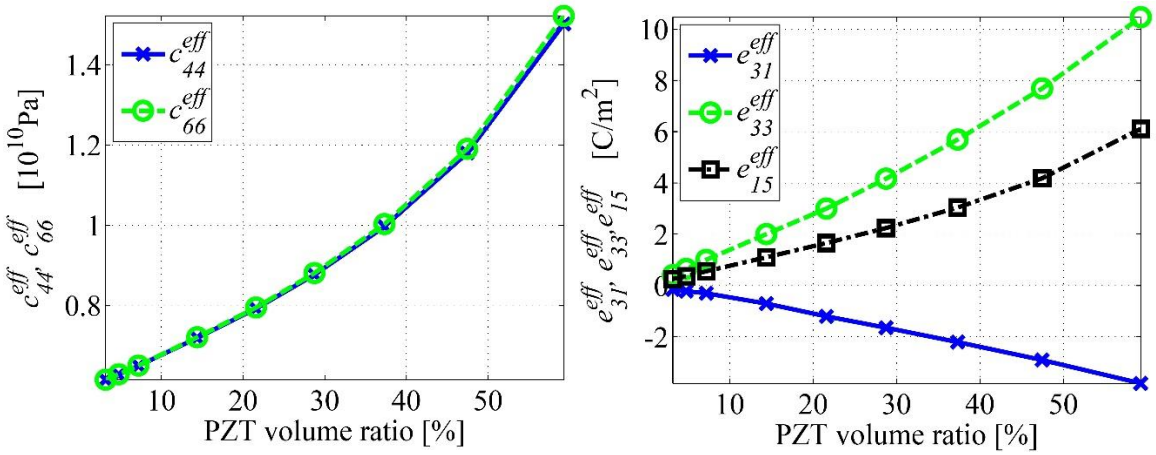

Figure 3. Variation of the effective (left) c_{44} and c_{66}, (right) e_{31}, e_{33} and e_{15} with PZT volume fraction in the smart ceramic composite

Figure 4 shows the effect of the PZT particle volume fraction on the effective dielectric (left) and thermal conductivity (right) material properties. One can observe that as the volume fraction increases, the effective dielectric and thermal conductivity coefficients decrease.

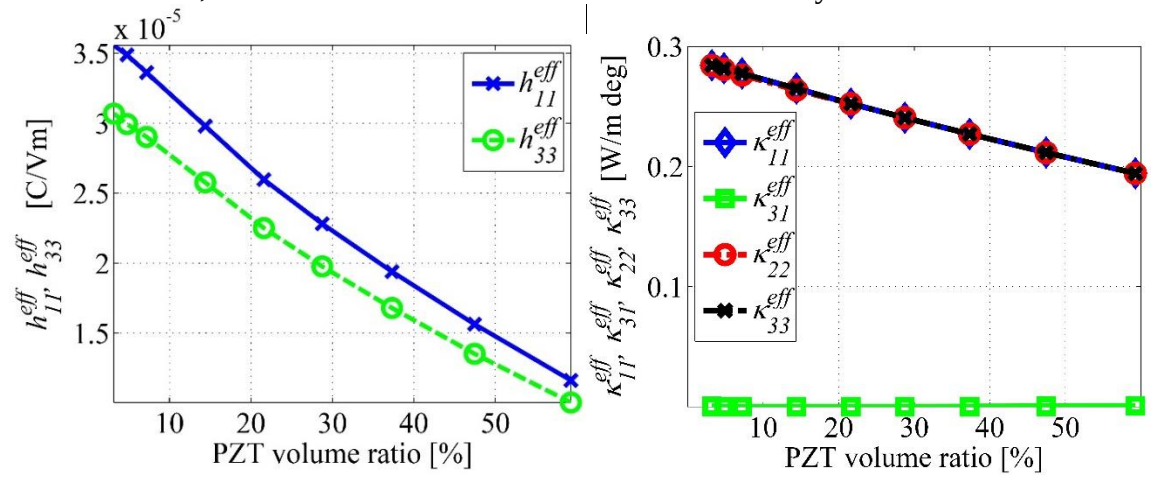

Figure 4. Variation of the effective (left) h_{11} and h_{33}, (right) k_{11}, k_{31}, k_{22} and k_{33} with PZT volume fraction in the smart ceramic composite

Conclusions

A finite element model of an RVE of cement-based piezoelectric composite is developed and applied to evaluate the effective elastic and piezoelectric material properties. The effect of the volume fraction of the piezoelectric particles on the effective thermo-electro-mechanical material properties of the composite are presented.

Acknowledgement

The authors gratefully acknowledge the supports by the Slovak Science and Technology Assistance Agency registered under number APVV-14-0216 and the Slovak Grant Agency VEGA-2/0046/16.

References

[1] Li, Z., Zhang, D. and Wu, K. (2001) Cement matrix 2-2 piezoelectric composite – part 1. Sensory effect, *Materials and Structures* **34**, 506–512.

[2] Dong, B. and Li, Z. (2005) Cement-based piezoelectric ceramic smart composites, *Composites Science and Technology* **65**, 1363–1371.
[3] Chaipanich, A. (2007) Effect of PZT particle size on dielectric and piezoelectric properties of PZT-cement composites, *Current Applied Physics* **7**, 574–577.
[4] Wang, F., Wang, H., Song, Y. and Sun, H. (2012) High piezoelectricity 0-3 cement-based piezoelectric composites, *Materials Letters* **76**, 208–210.
[5] Wu, T., Temizer, I. and Wriggers, P. (2013) Computational thermal homogenization of concrete, *Cement & Concrete Composites* **35**, 59–70.
[6] Mindlin, R.D. (1974) Equations of high frequency vibrations of thermopiezoelasticity problems, *International Journal of Solids and Structures* **10**, 625–637.
[7] Li, J.Y. and Dunn, M.L. (1998) Micromechanics of magnetoelectroelastic composite materials: average fields and effective behavior, *Journal of Intelligent Material Systems and Structures* **9**, 404–416.
[8] Xing, F., Dong, B. and Li, Z. (2008) Dielectric, piezoelectric, and elastic properties of cement-based piezoelectric ceramic composites, *Journal of American Society* **91**, 2886-2891.
[9] Saputra, A., Sladek, V., Sladek, J., Song, C. (2017) Micromechanics determination of effective material coefficients of cement-based piezoelectric ceramic composites. *Journal of Intelligent Material Systems and Structures* **29**(5), 845-862.